TESTING BSM HIGGS INTERACTIONS BY THE COMBINATION $(\kappa_V^2 - \kappa_{2V})$ IN HHjj PRODUCTION AT LHC

XVII CPAN DAYS VALENCIA - *November 19th – 21th, 2025*

Guillermo García Mir

(Universidad Autónoma de Madrid, IFT)

In collaboration with María José Herrero (UAM, IFT/UAM-CSIC), Daniel Domenech (UAM, IFT/UAM-CSIC)

Based on ArXiv : 2507.20988. To appear in PRD (2025)

We thank María Cepeda (CIEMAT) for her contribution in the first part of this work.

UNIVERSIDAD AUTONOMA DE MADRID

Instituto de Física Teórica UAM-CSIC

Motivation

★ Focus ⇒ BSM Higgs signals in **pp → HHjj** production process

★ Theoretical framework ⇒ predictions from **Higgs Effective Field Theory (HEFT)**

⇒ Most relevant effective coefficients to describe to describe BSM Higgs signals in **pp → HHjj** are **$a = \kappa_V$** & **$b = \kappa_{2V}$** (κ_λ is less relevant at large invariant mass M_{HH})

★ **MAIN ISSUE** ⇒ **pp → HHjj** provides access to the coefficient combination **$a^2 - b = \kappa_V^2 - \kappa_{2V}$** through the Vector Boson Fusion **(VBF)** subprocess.

★ Why is exploring this combination interesting?

⇒ **$(a^2 - b) \neq 0$** signals BSM Higgs physics

⇒ Different UV theories predict different values of this combination at low energy.

Several previous examples studied in the literature: example 2HDM (see Arco, Domenech, Herrero, Morales, Phys. Rev. D 108 (2023), 095013)

★ **FINAL GOAL** ⇒ study **sensitivity** to $(a^2 - b)$ in **pp → HHjj → $b\bar{b}\gamma\gamma jj$** at **HL–LHC.**

The Bosonic LO-HEFT Lagrangian

Only boson HEFT. Fermions as in SM

The Electroweak Chiral Lagrangian (for R_ξ covariant gauges):

- EW Gauge $SU(2)_L \times U(1)_Y$ & EW Chiral $SU(2)_L \times SU(2)_R$
- Operator ordering in **chiral dimension → Powers in momentum**

- GB fields $\boldsymbol{\omega_i}$ embedded in **exponential rep. U** $\quad U = e^{(i\frac{\omega^a \tau_a}{v})}$
- **U bi-doublet** under $SU(2)_L \times SU(2)_R$ $\quad U \to L U R^\dagger$

- Higgs field **H** introduced as a **singlet → generic polynomial** — **Uncorrelated Higgs couplings**

CHIRAL DIMENSION 2

$$\mathcal{L}^{\rm LO}_{\rm EChL} = \frac{v^2}{4}\left(1 + 2a\frac{H}{v} + b\frac{H^2}{v^2} + \dots\right)\mathrm{Tr}[D_\mu U^\dagger D^\mu U] - \frac{1}{2}m_H^2 H^2 - \kappa_3 \lambda v H^3 - \kappa_4 \frac{\lambda}{4} H^4$$

$$+\frac{1}{2}\partial_\mu H \partial^\mu H - \frac{1}{2g^2}\mathrm{Tr}[\hat{W}_{\mu\nu}\hat{W}^{\mu\nu}] - \frac{1}{2g'^2}\mathrm{Tr}[\hat{B}_{\mu\nu}\hat{B}^{\mu\nu}] + \mathcal{L}_{GF} + \mathcal{L}_{FP}$$

Triple and quartic Higgs self-interaction

(SM scenario: $a = b = \kappa_3 = \kappa_4 = 1$) **Anomalous couplings: parametrize possible BSM effects in LO-HEFT**

HEFT HVV & HHVV effective couplings:

Connection with κ-formalism only in Unitary gauge.

HVV

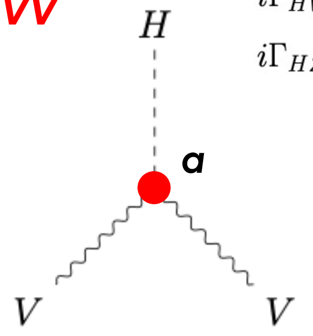

$$i\Gamma_{HWW} = i a g m_W g_{\mu\nu}$$
$$i\Gamma_{HZZ} = i a \frac{g}{\cos\theta_W} m_Z g_{\mu\nu}$$

$\boldsymbol{a = \kappa_V}$

ATLAS (95%CL) $\kappa_V \in [0.99 – 1.11]$

ATLAS Collaboration, Nature 607 (2022) 52

CMS (95%CL) $\kappa_V \in [0.97 – 1.09]$

CMS Collaboration, Nature 607 (2022) 60

HHVV

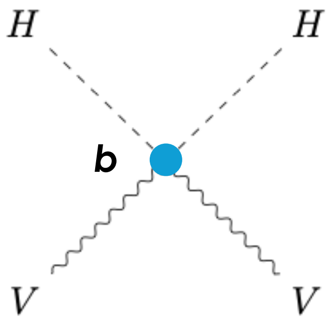

$$i\Gamma_{HHWW} = i b \frac{g^2}{2} g_{\mu\nu}$$
$$i\Gamma_{HHZZ} = i b \frac{g^2}{2\cos\theta_W^2} g_{\mu\nu}$$

$\boldsymbol{b = \kappa_{2V}}$

ATLAS (95%CL) $\kappa_{2V} \in [0.6 – 1.5]$

ATLAS Collab., Phys. Rev. Lett. 133 (2024) 101801

CMS (95%CL) $\kappa_{2V} \in [0.6 – 1.4]$

CMS Collab., Phys. Lett. B 861 (2025) 139210

The WW→HH subprocess at LO-HEFT

WW → HH diagrams in <u>unitary gauge</u> (assuming $\kappa_3 = \kappa_4 = 1$):

s-channel

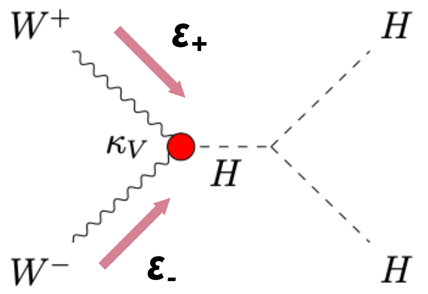

$$\mathcal{A}_s = a\frac{3g^2}{2}\frac{m_H^2}{s-m_H^2}(\epsilon_+\cdot\epsilon_-)$$

W± polarizations

c-channel

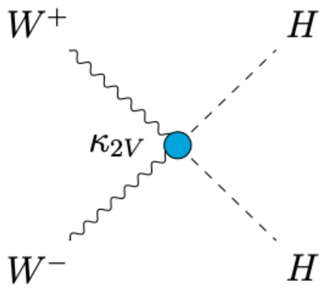

$$\mathcal{A}_c = b\frac{g^2}{2}(\epsilon_+\cdot\epsilon_-)$$

κ_{2V} only accessible in HH production

t-channel

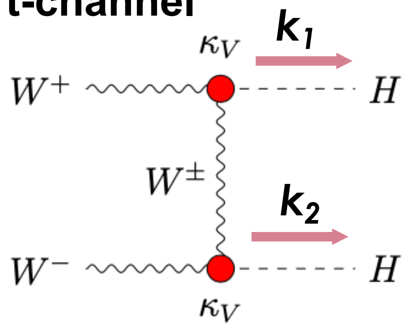

u-channel

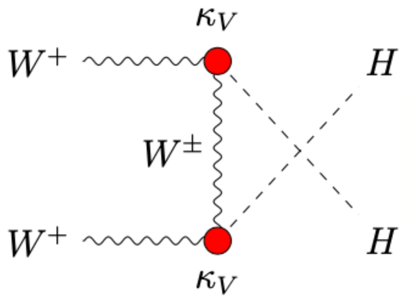

Gauge invariant scattering amplitude:

$$\mathcal{A} = \mathcal{A}_c + \mathcal{A}_s + \mathcal{A}_t + \mathcal{A}_u$$

$$\mathcal{A}_t = a^2 g^2\frac{m_W^2(\epsilon_+\cdot\epsilon_-)+(\epsilon_+\cdot k_1)(\epsilon_+\cdot k_2)}{t-m_W^2}$$

Higgs 4-momenta

$$\mathcal{A}_u = a^2 g^2\frac{m_W^2(\epsilon_+\cdot\epsilon_-)+(\epsilon_+\cdot k_2)(\epsilon_+\cdot k_1)}{u-m_W^2}$$

Connection with κ-formalism only in Unitary gauge.

BSM parametrization must preserve Gauge Invariance in the Lagrangian:

HEFT κ-formalism

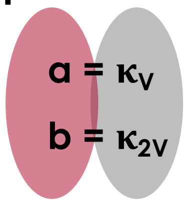

SM-VBF predictions recovered for a = b = 1 ($\kappa_V = \kappa_{2V} = 1$).

BSM-VBF emerge has a ≠ b ≠ 1 ($\kappa_V \neq \kappa_{2V} \neq 1$).

The role of $(a^2 - b)$ in $WW \to HH$ within HEFT

High energy dominant helicity amplitude is $\mathcal{A}^L$:

In the limit $\sqrt{s} \gg M_W, M_H$ ($\sqrt{s} \simeq$ TeV) $\rightarrow$ clear dominance of **longitudinal modes helicity** ($\varepsilon_\pm \rightarrow \varepsilon_\pm^L$):

$$\mathcal{A}^L = \mathcal{A}(W_L^+ W_L^- \to HH)$$

$$\mathcal{A}^L = \mathcal{A}^L_s + \mathcal{A}^L_c + \mathcal{A}^L_t + \mathcal{A}^L_u$$

$$\mathcal{A}^L_s = \mathcal{O}(s^0) \qquad \mathcal{A}^L_t = a^2 g^2 \frac{1}{8m_W^2}(1-\cos\theta)\, s + O(s^0)$$

$$\mathcal{A}^L_c = -b\frac{g^2}{4m_W^2} s + \mathcal{O}(s^0) \qquad \mathcal{A}^L_u = a^2 g^2 \frac{1}{8m_W^2}(1+\cos\theta)\, s + O(s^0)$$

$$\mathcal{A}^L = (a^2 - b)\, \frac{g^2}{8m_W^2} s + \mathcal{O}(s^0)$$

IN HEFT: FOR $\sqrt{s} \gg M_W, M_H$ AMPLITUDE GROWS WITH s AND IS PROPORTIONAL TO $a^2 - b$

$WW \rightarrow HH$ high energy total unpolarized cross-section:

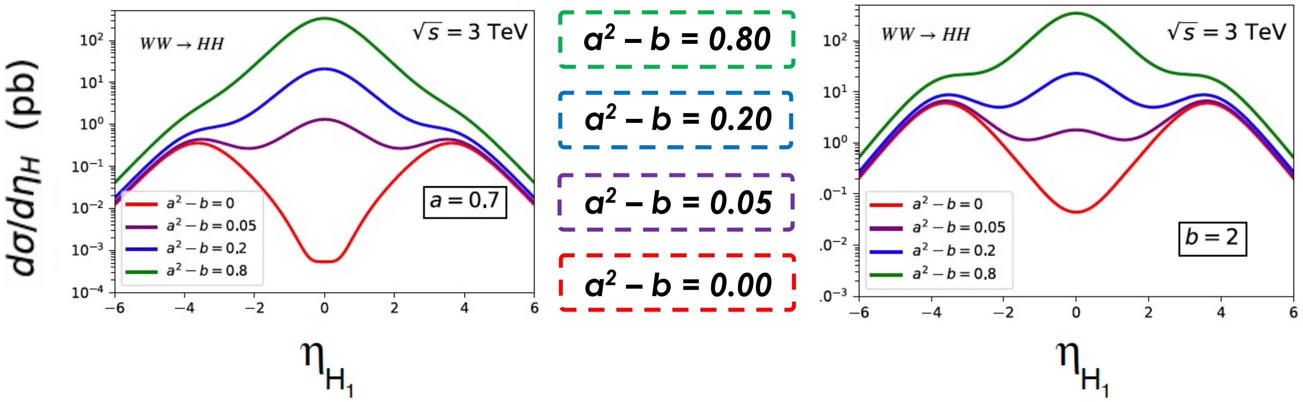

$$\frac{d\sigma}{d\cos\theta} = \frac{1}{64\pi s}\frac{\sqrt{s-4m_H^2}}{\sqrt{s-4m_V^2}}|\bar{\mathcal{A}}|^2 \qquad \frac{d\sigma}{d\eta} = \frac{1}{\cosh^2\eta}\frac{\sqrt{s-4m_H^2}}{\sqrt{s-4m_V^2}}|\bar{\mathcal{A}}|^2$$

CENTRAL PEAK shaping in angular distributions:

$\frac{d\sigma}{d\eta}, \frac{d\sigma}{d\cos\theta} \rightarrow$ **dominance increasing with $a^2 - b$**

Exploring pp → HHjj: The VBF selection strategy

pp → HHjj parton level topologies:

Double Higgs-strahlung

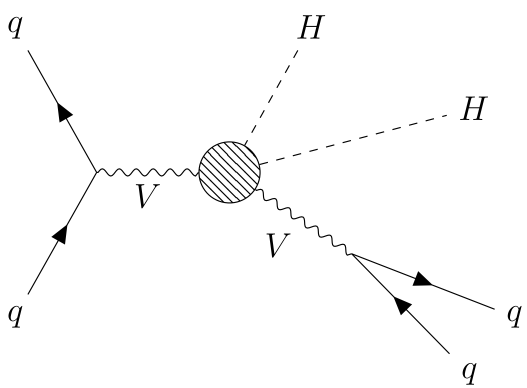

Vector boson fusion (VBF)

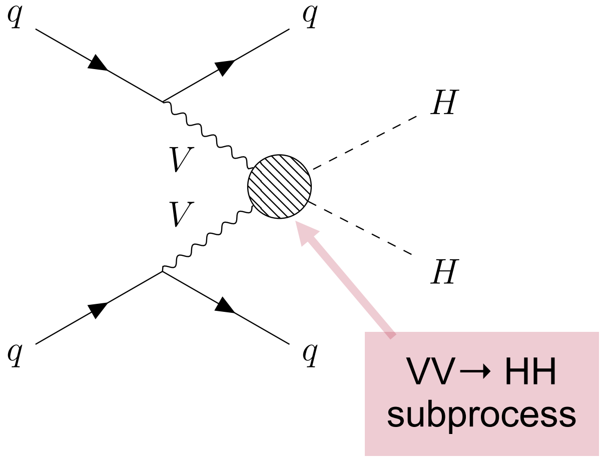

⇒ **VBF characteristics of jj' pair:**

- Two narrow jet cones
- Opposite hemispheres
- Large $\Delta\eta_{jj'} = |\eta_j - \eta_{j'}| \gtrsim 4$
- Large $m_{jj'} > 500$ GeV

VBF selection strategy:

VBF topology	$P_{T,j} > 20{,}0$ GeV	$2 < \lvert\eta_j\rvert < 5$	$\eta_j \times \eta_{j'} < 0$
	$m_{jj'} > 500$ GeV	$\Delta R_{jj} > 0{,}4$	

$$\Delta R_{AB} = \sqrt{(\Delta\eta_{AB})^2 + (\Delta\Phi_{AB})^2}$$

VBF selection strategy acceptance:

50% - 75% for the case of **HEFT**

depending on a & b values

*50% for the SM case

Feynman diagrams contributing to pp → HHjj within HEFT

Parton level simulations tools:

MADGRAPH 5
[10.1007/jhep07(2014)079]

HEFT coefficients: ● $a = \kappa_V$ ● $b = \kappa_{2V}$

(SM scenario: a = b = 1)

Double Higgs-strahlung

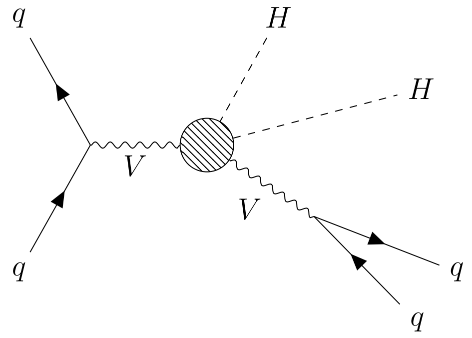

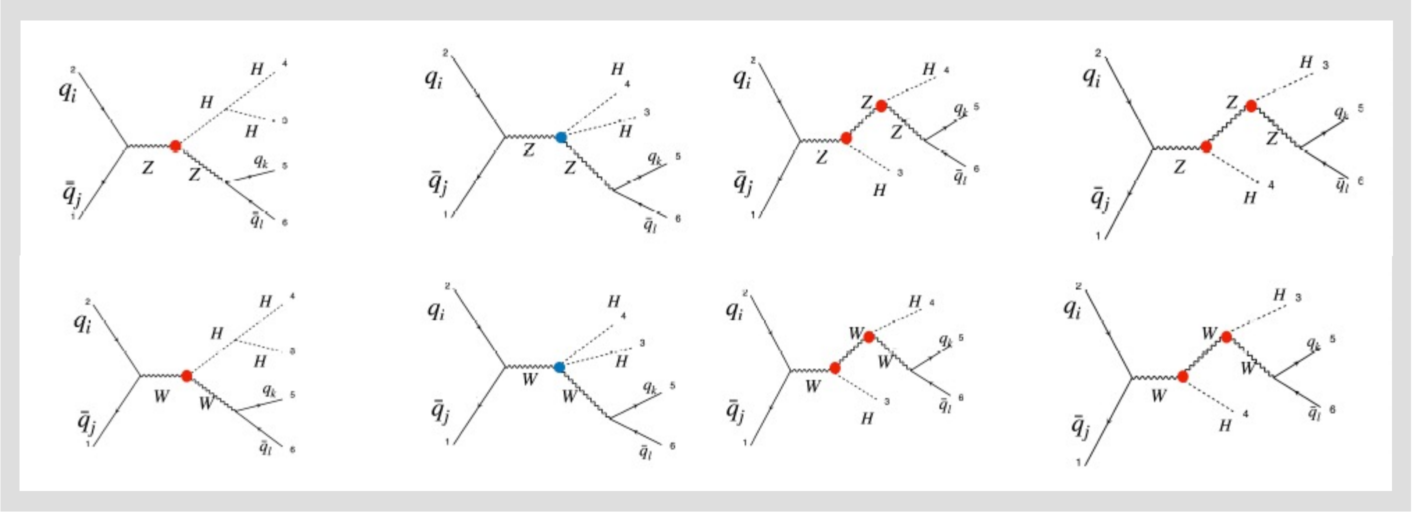

Vector boson fusión (VBF)

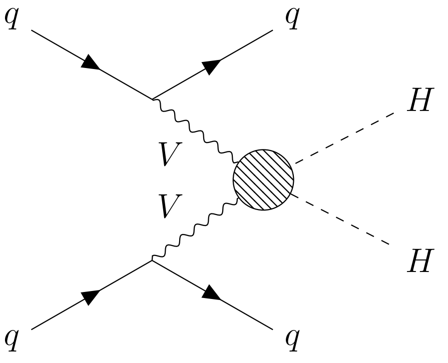

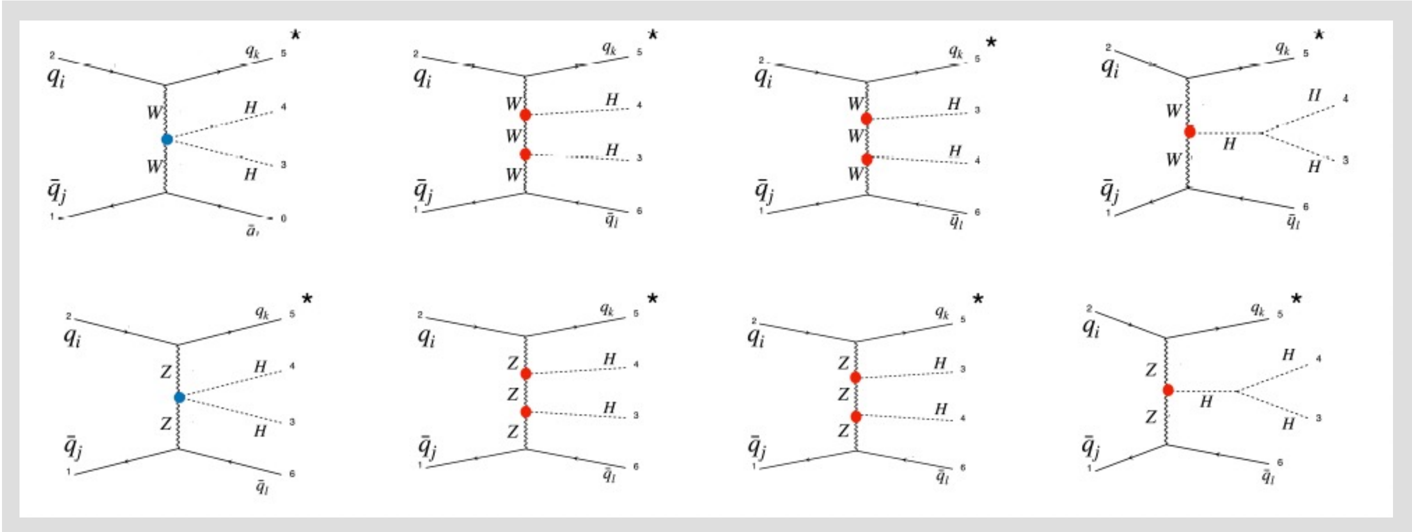

HEFT results on the total xsection $\sigma(pp \rightarrow HHjj)$ as a function of $(a^2 - b)$

THE MOST SENSITIVE PARAMETER IS (a^2 – b)

LARGEST VALUES OF (a^2 – b) = LARGEST VALUES OF σ

Cross section for the SM at LHC:

$\sigma_{SM}(pp \rightarrow HHjj) = 8 \cdot 10^{-4}$ pb

Parton-level results (Madgraph 5)

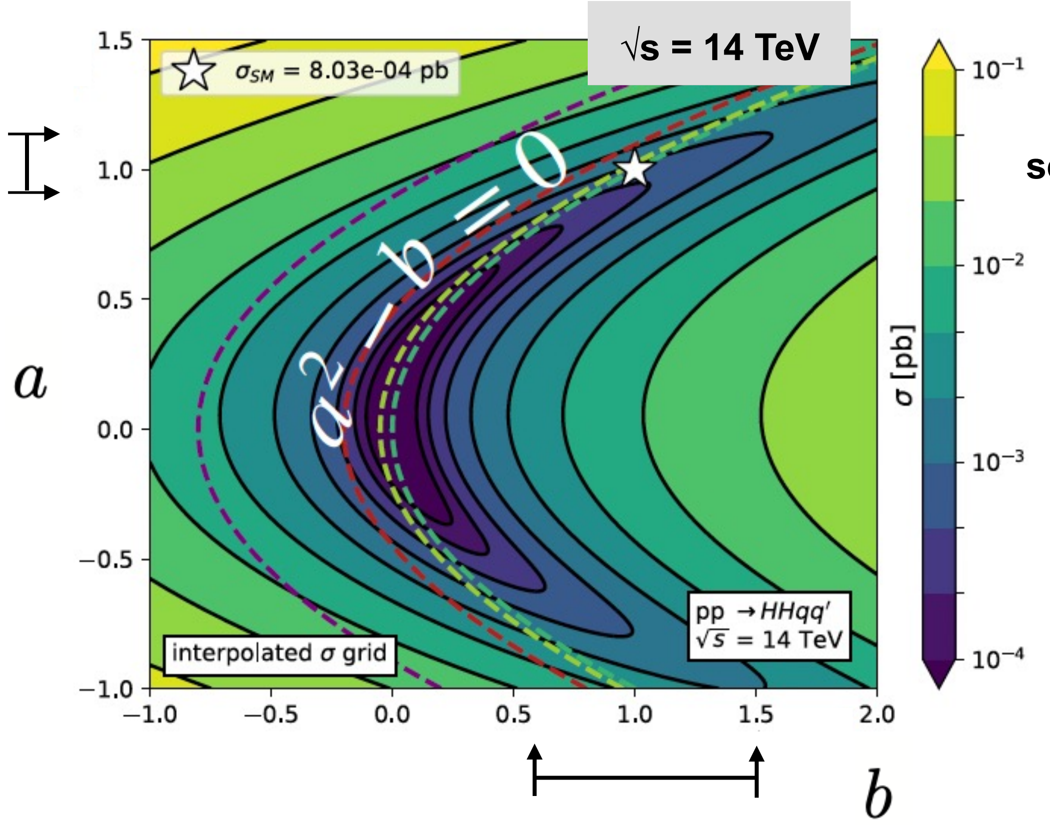

Boomerang cross-section contour lines following (a^2 – b)

$a^2 - b$

$a^2 - b = 0.80$

$a^2 - b = 0.20$

$a^2 - b = 0.05$

$a^2 - b = 0.00$

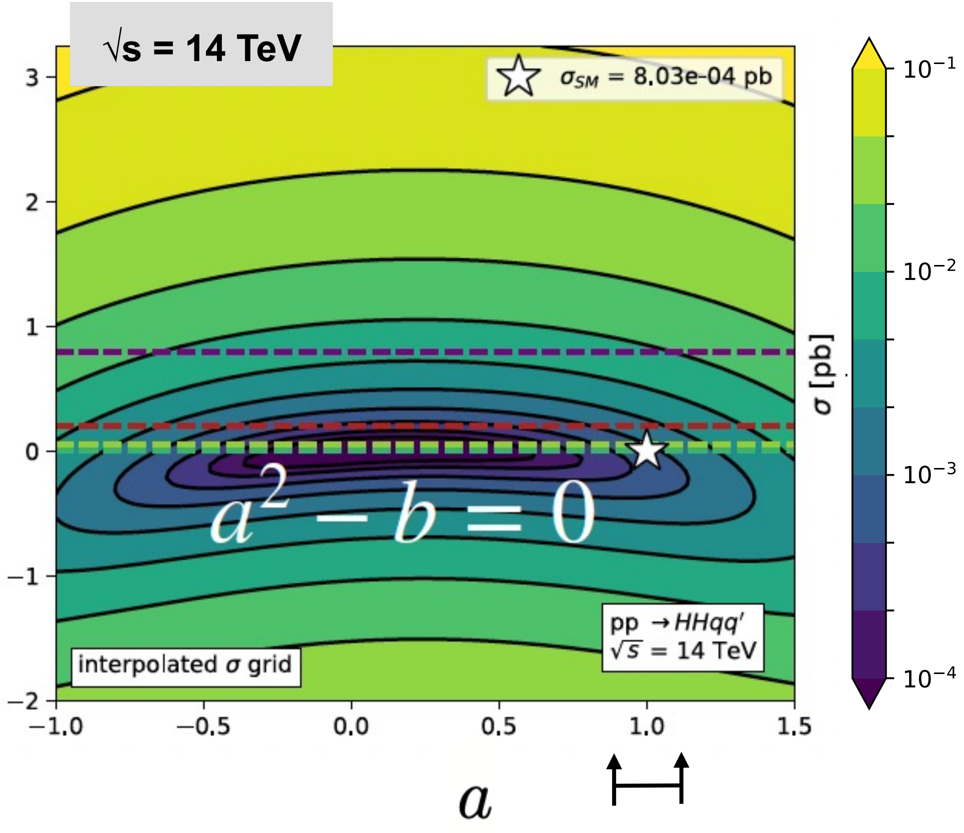

Interpolated function σ(a, b):

$$\sigma_{pp\to HHjj'}(a,b) = C_{a^4}a^4 + C_{a^3}a^3 + C_{a^2}a^2 + C_{a^2b}a^2b + C_{ab}ab + C_{b^2}b^2$$

$$C_{a^4} = 1{,}62 \times 10^{-2}pb, \quad C_{a^3} = -0{,}41 \times 10^{-2}pb, \quad C_{a^2} = 0{,}05 \times 10^{-2}pb$$
$$C_{a^2b} = -2{,}41 \times 10^{-2}pb, \quad C_{ab} = 0{,}26 \times 10^{-2}pb, \quad C_{b^2} = 0{,}93 \times 10^{-2}pb$$

HEFT results on the diff. cross section $\frac{d\sigma(pp \to HHjj)}{d\eta_H}$ for $(a^2 - b) \neq 0$

HIGGS BOSON TRANSVERSALITY (η = 0) DETERMINED BY THE COMBINATION $a^2 - b$

$a = \kappa_V = 1.00$

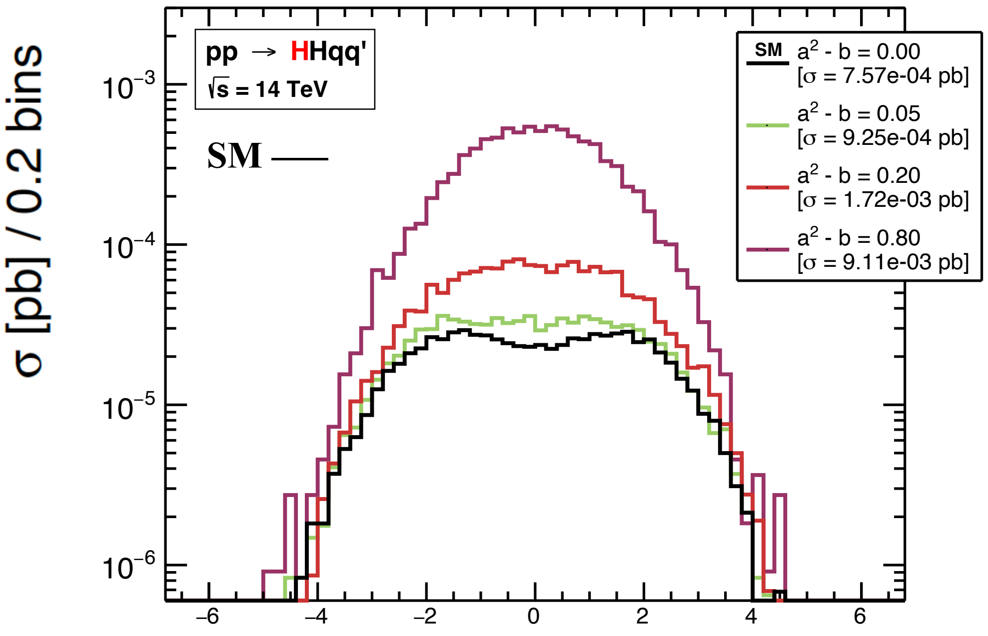

$a = \kappa_V = 0.97$

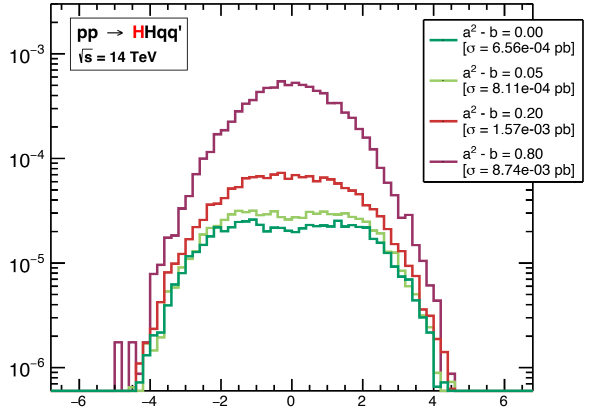

$a = \kappa_V = 0.90$

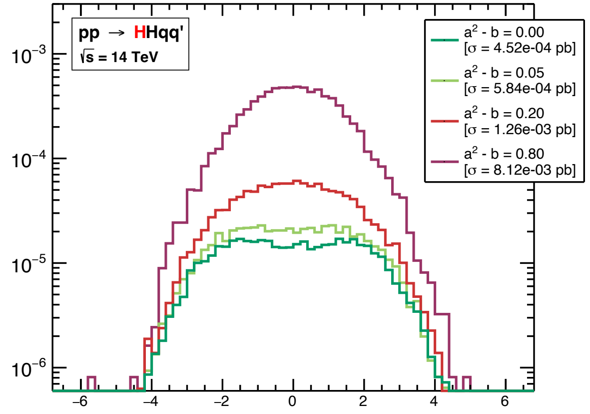

Central peak (η = 0) dominant for larger $(\kappa_V^2 - \kappa_{2V}) \neq 0$

$b = \kappa_{2V} = 1.00$

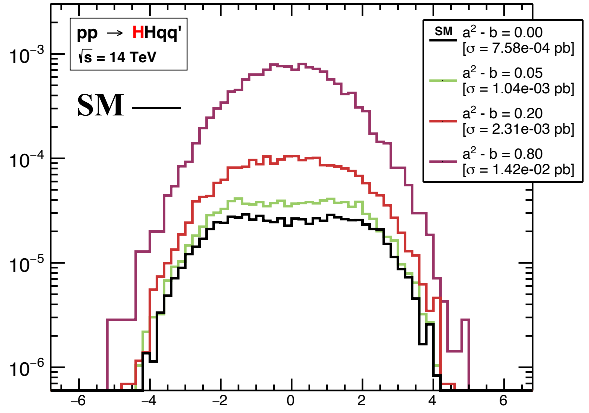

$b = \kappa_{2V} = 1.50$

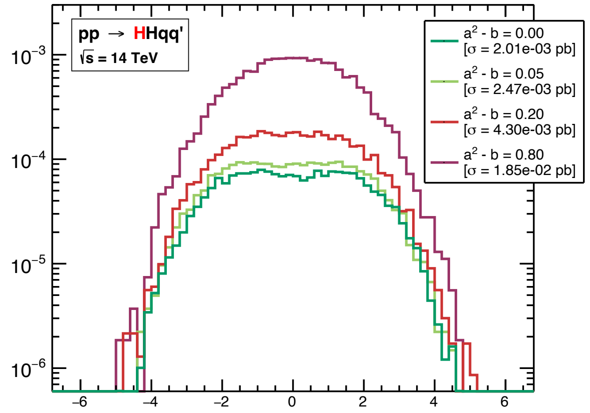

Parton-level results (Madgraph 5)

Two peaks at $|\eta_H| \simeq \pm 2$ when $(\kappa_V^2 - \kappa_{2V}) = 0$

$a^2 - b = 0.80$ | *$a^2 - b = 0.20$* | *$a^2 - b = 0.05$* | *$a^2 - b = 0.00$*

Detector-level strategy for pp → HHjj → $b\bar{b}\gamma\gamma jj$ final state within HEFT

$b\bar{b}\gamma\gamma jj$ final state:

BR(HH → $b\bar{b}\gamma\gamma$) = 1.3×10^{-3}

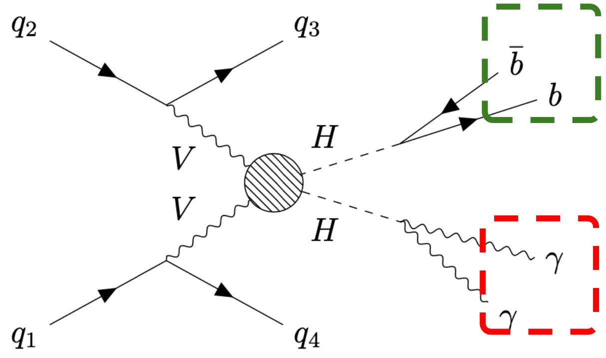

Comparatively less background than others ($b\bar{b}b\bar{b}$, $b\bar{b}\tau^+\tau^-$…)

&

High detecting resolution of $\gamma\gamma$

Detector-level simulation tools:

Hadronization and parton showering:

Modelled by: ***PYTHIA v8.235*** *[arXiv:1410.3012]*

Jet clustering algorithm: ***anti-k$_t$*** *[arXiv:0802.1189v2]* *(FASTJET package [arXiv:1111.6097v1])*

Phase-2 upgraded CMS detector:

Fast and parametric detector simulation: ***DELPHES 3*** *[arXiv:1307.6346v3]*

Detector-level $b\bar{b}\gamma\gamma jj$ selection strategy:

VBF criteria (and b-jet/γ identification)

$$E_i = \frac{N_i^{\text{detector-level}}}{N^{\text{parton-level}}}$$

≥ 2 light jets: $P_{T,j} > 20$ GeV, $2 < \lvert\eta_j\rvert < 5$
VBF jet pair jj' maximizes ΔR
$\eta_j \times \eta_{j'} < 0$
$m_{jj'} > 500$ GeV

≥ 2 "loose" photons: $P_{T,\gamma} > 18$ GeV, $\lvert\eta_\gamma\rvert < 2{,}5$
Photon pair $\gamma\gamma$ closest to $m_{\gamma\gamma} = m_H = 125$ GeV
≥ 2 "loosely" b-tagged jets: $P_{T,j_b} > 25$ GeV, $\lvert\eta_{j_b}\rvert < 2{,}5$
b-jet pair $j_b j_{\bar{b}}$ closest to $m_{j_b j_{\bar{b}}} = m_H = 125$ GeV

Total efficiency

Total selection efficiency ($\Pi^i E_i$)	36 % – 44 %

	$a = 1{,}00$							
$a^2 - b$	$-1{,}00$	$-0{,}80$	$0{,}00$ (SM)	$0{,}05$	$0{,}20$	$0{,}80$	$1{,}00$	$1{,}50$
$\Pi^i E_i$	44 %	44 %	36 %	36 %	39 %	41 %	41 %	43 %

TOTAL EFFICIENCY INCREASES WITH $\lvert(a^2 - b)\rvert$

BSM $b\bar{b}\gamma\gamma jj$ signal rates at HL-LHC within HEFT as a function of $(a^2 - b)$

HL-LHC operation benchmarks:

L_{int} = 3000 fb^{-1} Pu_{avg} = 200 $\sqrt{s}$ = 14 TeV

	$a = 1.00$							
$a^2 - b$	-1.00	-0.80	0.00 (SM)	0.05	0.20	0.80	1.00	1.50
$\sigma[pb]$	$1{,}25\times10^{-5}$	$7{,}66\times10^{-6}$	$9{,}54\times10^{-7}$	$1{,}22\times10^{-6}$	$2{,}49\times10^{-6}$	$1{,}49\times10^{-5}$	$2{,}17\times10^{-5}$	$4{,}39\times10^{-5}$
$\Pi^i E_i$	44%	44%	36%	36%	39%	41%	41%	43%
N	16	10	1.0	1.3	2.9	18	27	56

	$a = 0.97$				$a = 0.90$			
$a^2 - b$	0.00	0.05	0.20	0.80	0.00	0.05	0.20	0.80
$\sigma[pb]$	$8{,}12\times10^{-7}$	$1{,}06\times10^{-6}$	$2{,}28\times10^{-6}$	$1{,}44\times10^{-5}$	$5{,}55\times10^{-7}$	$7{,}55\times10^{-7}$	$1{,}85\times10^{-6}$	$1{,}34\times10^{-5}$
$\Pi^i E_i$	36%	36%	38%	41%	35%	37%	38%	42%
N	0.87	1.1	2.6	18	0.58	0.84	2.1	17

	$b = 1.00$				$b = 1.50$			
$a^2 - b$	0.00 (SM)	0.05	0.20	0.80	0.00	0.05	0.20	0.80
$\sigma[pb]$	$9{,}47\times10^{-7}$	$1{,}36\times10^{-6}$	$3{,}34\times10^{-6}$	$2{,}24\times10^{-5}$	$2{,}64\times10^{-6}$	$3{,}33\times10^{-6}$	$6{,}07\times10^{-6}$	$2{,}89\times10^{-5}$
$\Pi^i E_i$	35%	35%	39%	40%	36%	36%	36%	40%
N	1.0	1.4	3.9	27	2.8	3.6	6.6	34

*After introducing detector-level $b\bar{b}\gamma\gamma jj$ selection strategy

Characteristic shapes of BSM HEFT signals: $\eta_{\gamma\gamma}$ diff. xsection

$\eta_{\gamma\gamma}$ SHAPES NOT AFFECTED by the simulated detector effects in $b\bar{b}\gamma\gamma jj$ final state

$a = \kappa_V = 1.00$

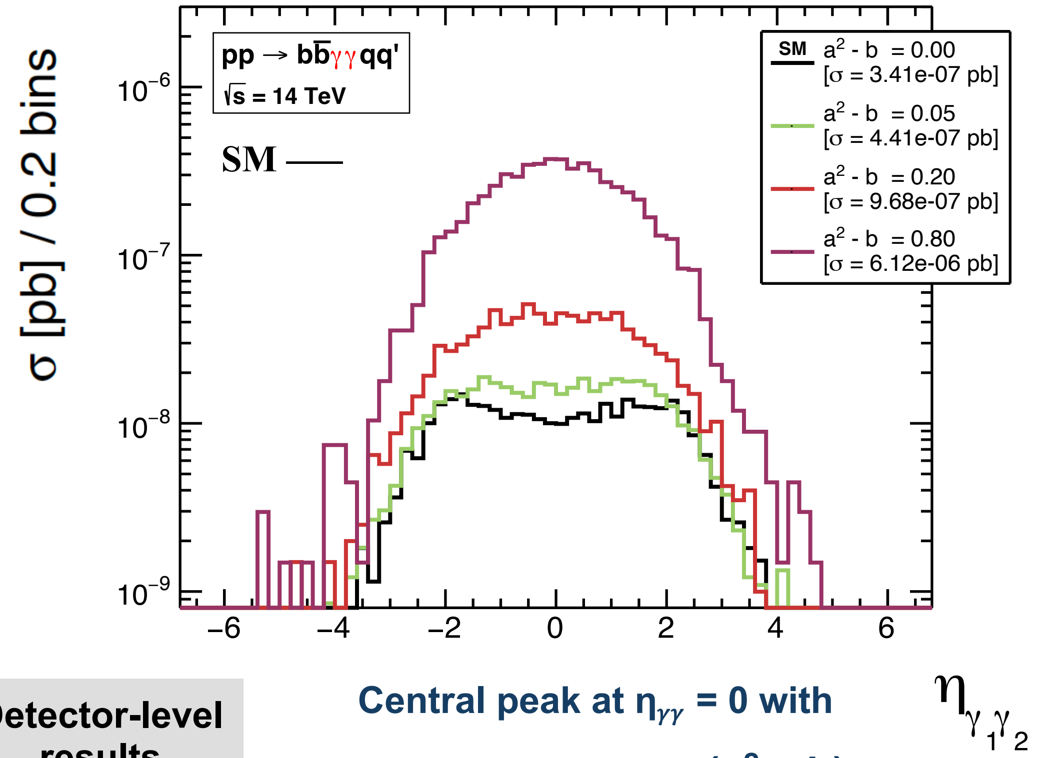

Detector-level results

Central peak at $\eta_{\gamma\gamma} = 0$ with height growing with $(a^2 - b)$ in contrast to SM (black)

$a = \kappa_V = 0.97$

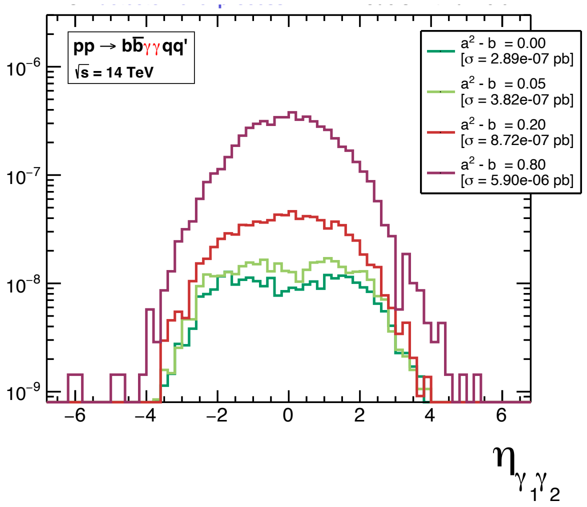

$a = \kappa_V = 0.90$

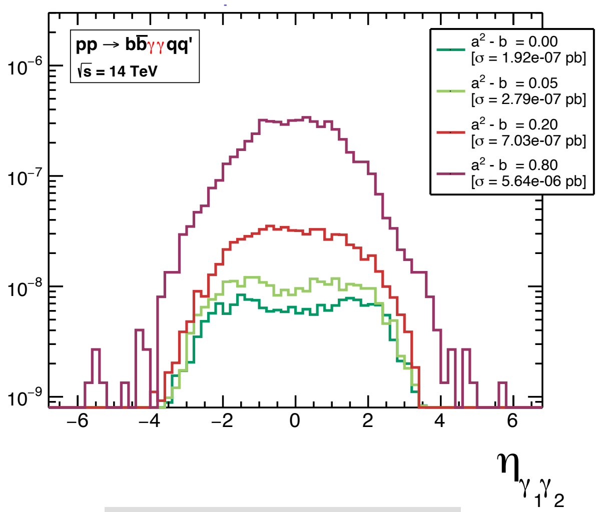

$b = \kappa_{2V} = 1.00$

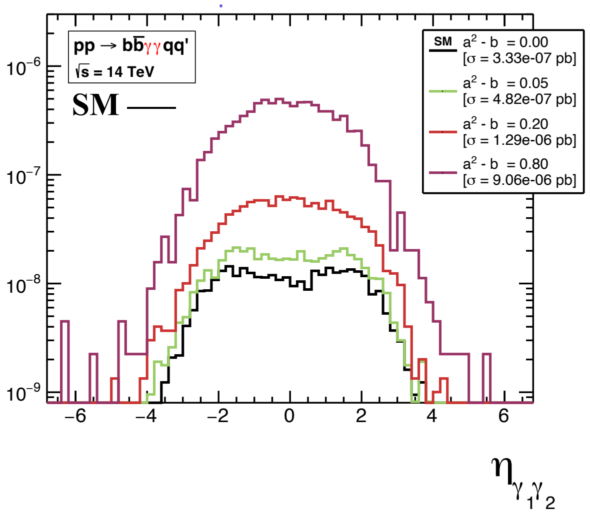

$b = \kappa_{2V} = 1.50$

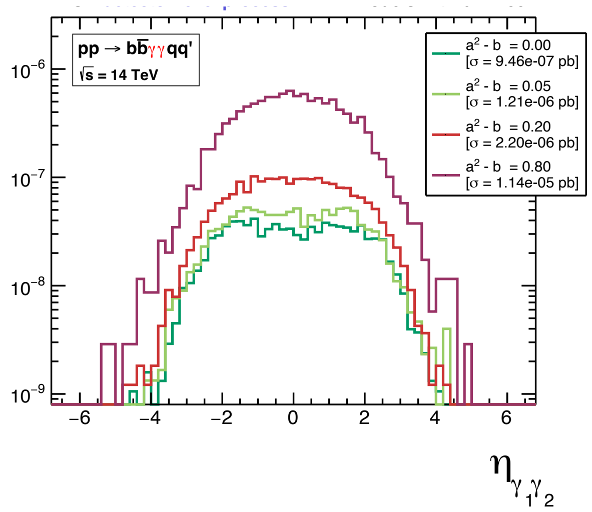

Characteristic shapes of BSM HEFT signals: η_{bb} diff. xsection

η_{bb} shapes NOT AFFECTED by the simulated detector effects in $b\bar{b}\gamma\gamma jj$ final state

$a = \kappa_V = 1.00$

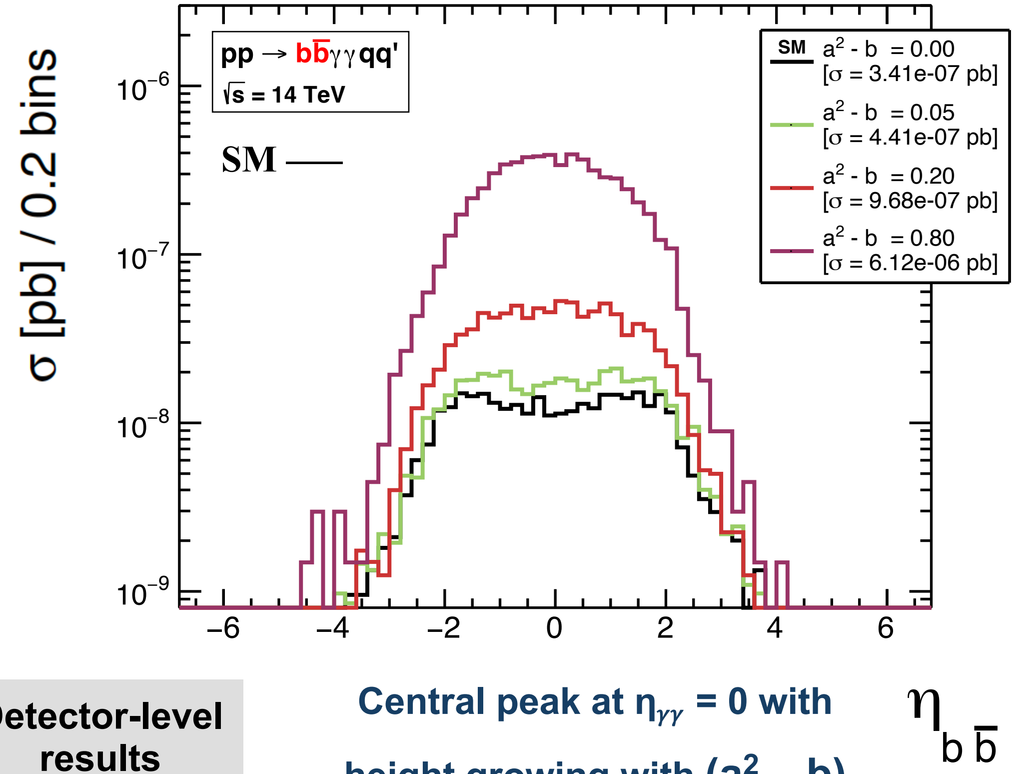

Detector-level results

Central peak at $\eta_{\gamma\gamma} = 0$ with height growing with $(a^2 - b)$ in contrast to SM (black)

$a = \kappa_V = 0.97$

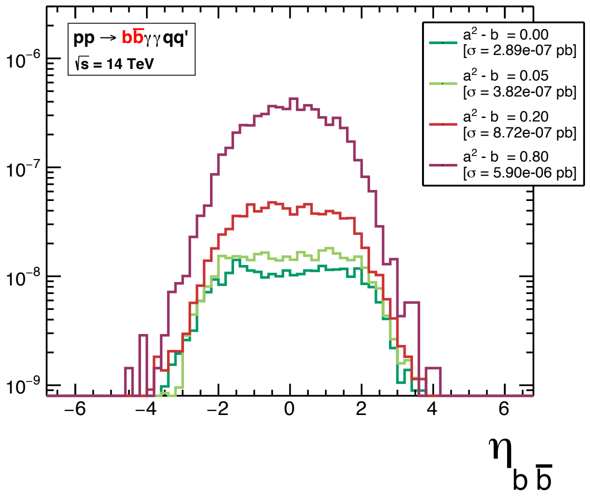

$a = \kappa_V = 0.90$

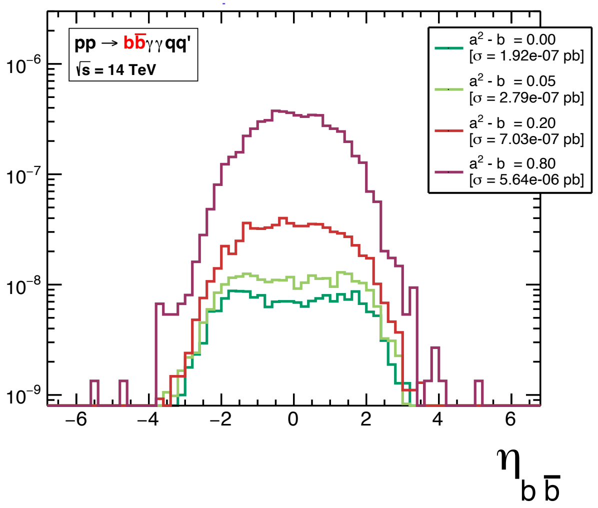

$b = \kappa_{2V} = 1.00$

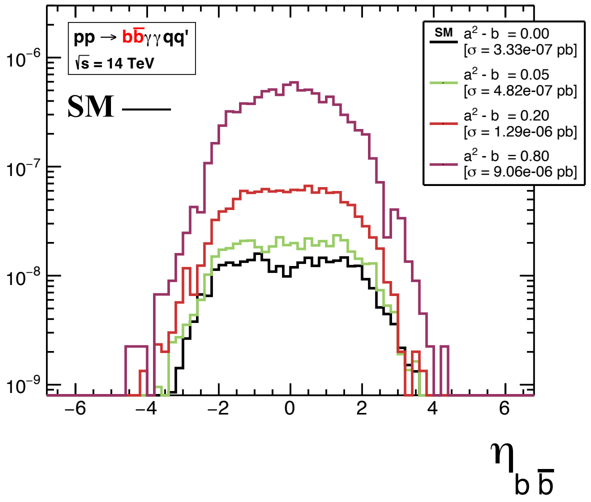

$b = \kappa_{2V} = 1.50$

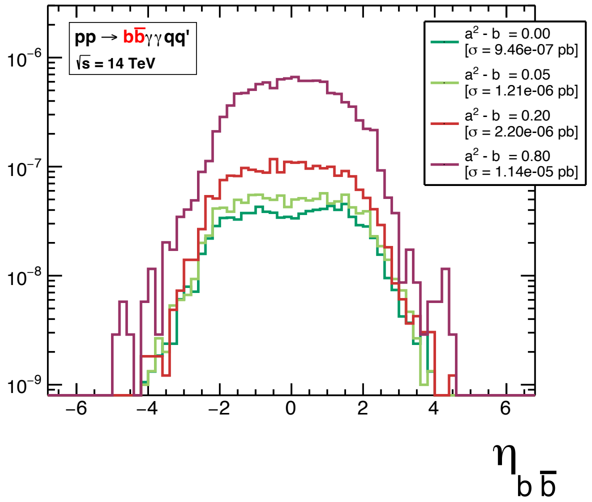

Characteristic shapes of BSM HEFT signals: $m_{\gamma\gamma bb}$ diff. xsection

LARGER ENHACEMENT at HIGH INVARIANT MASS $M_{b\bar{b}\gamma\gamma}$ for GREATER $a^2 - b$

$a = \kappa_V = 1.00$

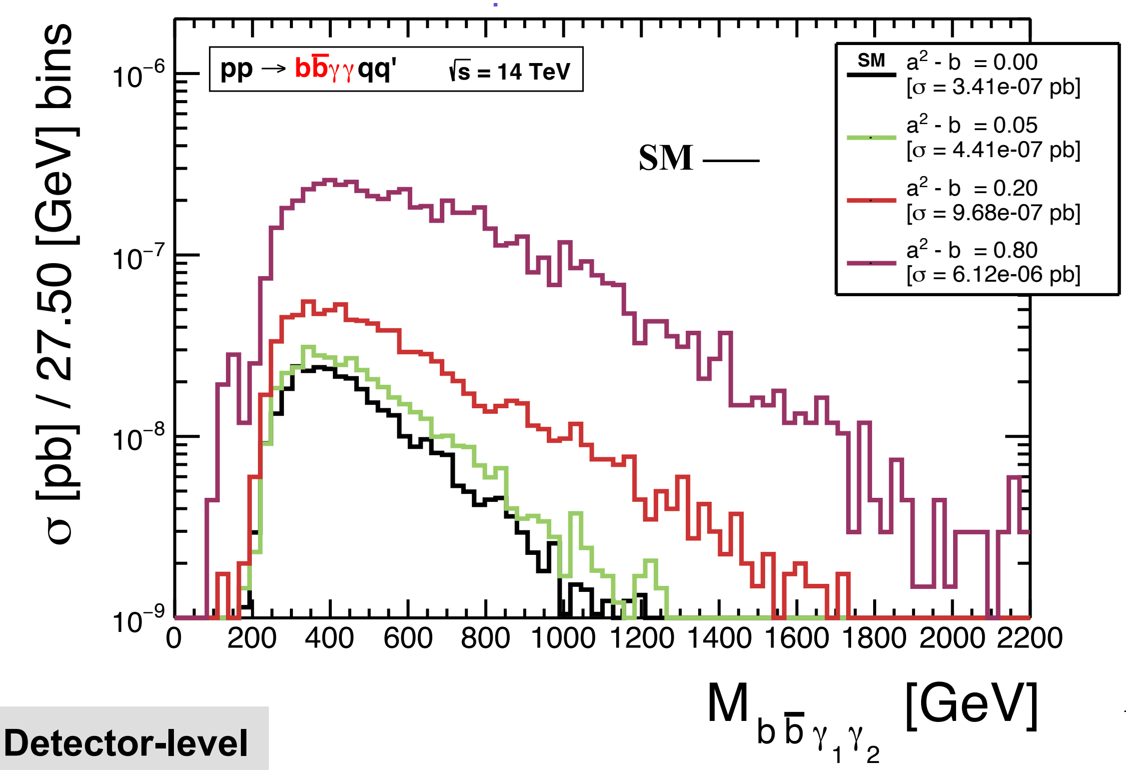

$a = \kappa_V = 0.97$

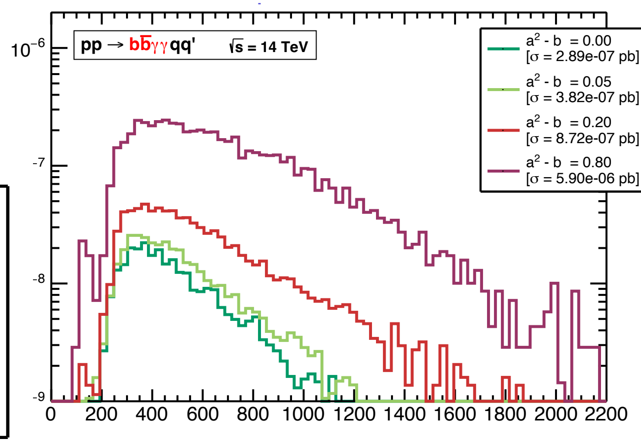

$a = \kappa_V = 0.90$

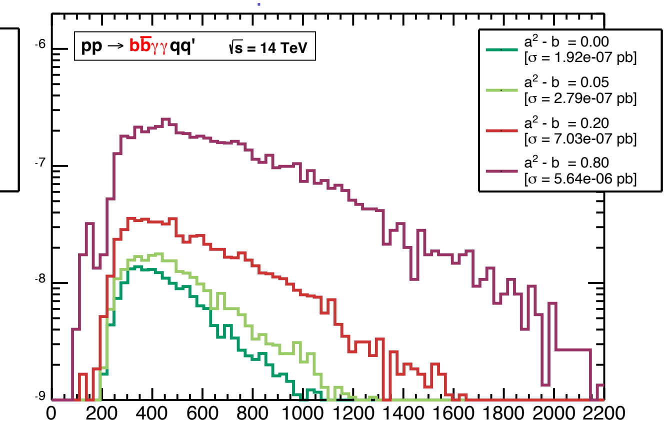

$b = \kappa_{2V} = 1.00$

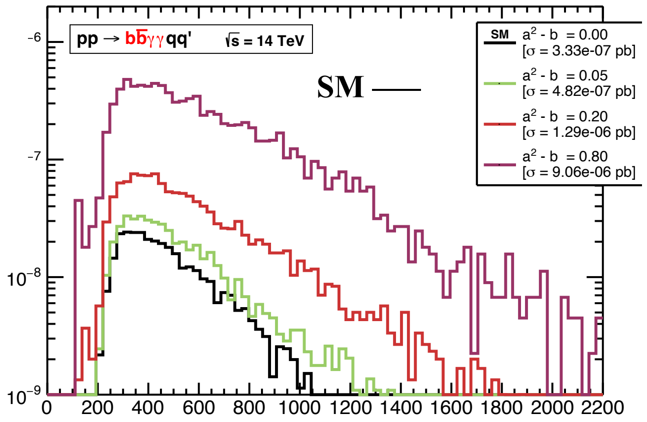

$b = \kappa_{2V} = 1.50$

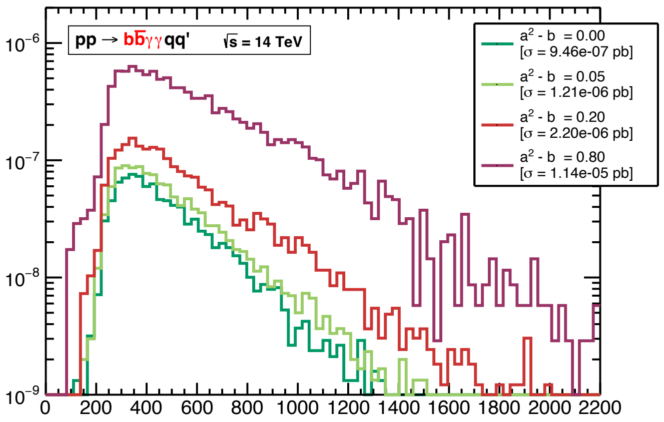

Detector-level results

$a^2 - b = 0.80$ | *$a^2 - b = 0.20$* | *$a^2 - b = 0.05$* | *$a^2 - b = 0.00$*

Comparing the size of Signal/Background in $b\bar{b}\gamma\gamma jj$ final state

Parton-level results (Madgraph 5)

HEFT

$\sigma(\gamma\gamma b\bar{b}jj)$(pb): BSM signal versus SM background rates (parton level)

Cuts applied: $p_{T_j} \geq 20$ GeV, $2 < |\eta_j| < 5$, $\eta_{j_1} \cdot \eta_{j_2} < 0$, $\Delta R_{jj} > 0.4$, $M_{jj} > 500$ GeV

Additional cuts in SM-QCD-EW (non resonant) background: $M_{b\bar{b}} > 100$ GeV, $M_{\gamma\gamma} > 100$ GeV

BSM Signal ($a^2 - b \neq 0$) $\gamma\gamma b\bar{b}jj$ via $HHjj$		SM-EW ($\mathcal{O}(\alpha^3\hbar^0)$) $\gamma\gamma b\bar{b}jj$ via $HHjj$	SM-QCD-EW ($\mathcal{O}(\alpha_s^2\alpha^1\hbar^0)$) $\gamma\gamma b\bar{b}jj$ (non-resonant)	SM-QCD-EW ($\mathcal{O}(\alpha_s^2\alpha^3\hbar^1)$) $\gamma\gamma b\bar{b}jj$ via HH from ggF	SM-EW ($\mathcal{O}(\alpha^3\hbar^0)$) $\gamma\gamma b\bar{b}jj$ via $ZHjj$
$a^2 - b$ ($a = 1$)		**Tree-level**	**Tree-level**	**One-loop**	**Tree-level**
0.2	2.2×10^{-6}	9.8×10^{-7}	8.1×10^{-4} **DOMINANT BKG**	4.7×10^{-7}	3.6×10^{-8}
0.8	1.2×10^{-5}				
1	2.2×10^{-5}				
-1	7.4×10^{-5}				

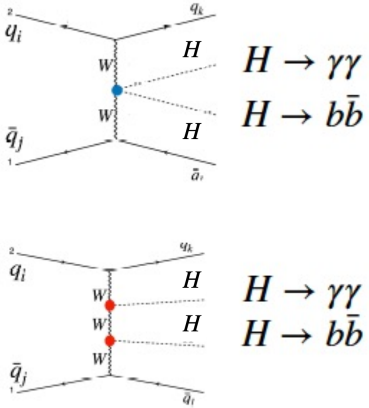

+ ...

SAME AS HEFT
WITH a = b = 1

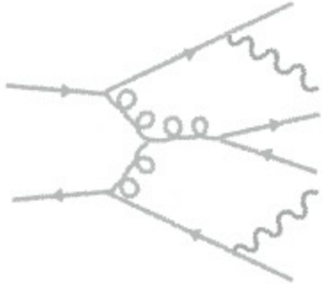

+ ...

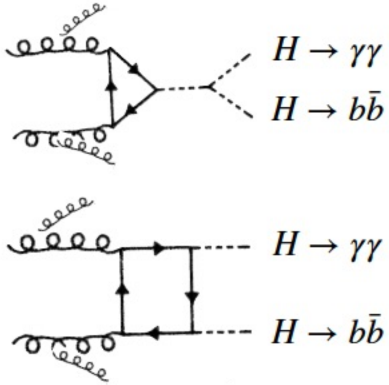

+ ...

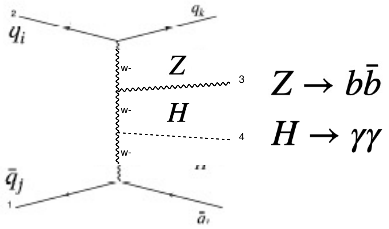

+ ...

Further signal-background discrimination strategies

BKG & HEFT differential cross-section distribution comparison

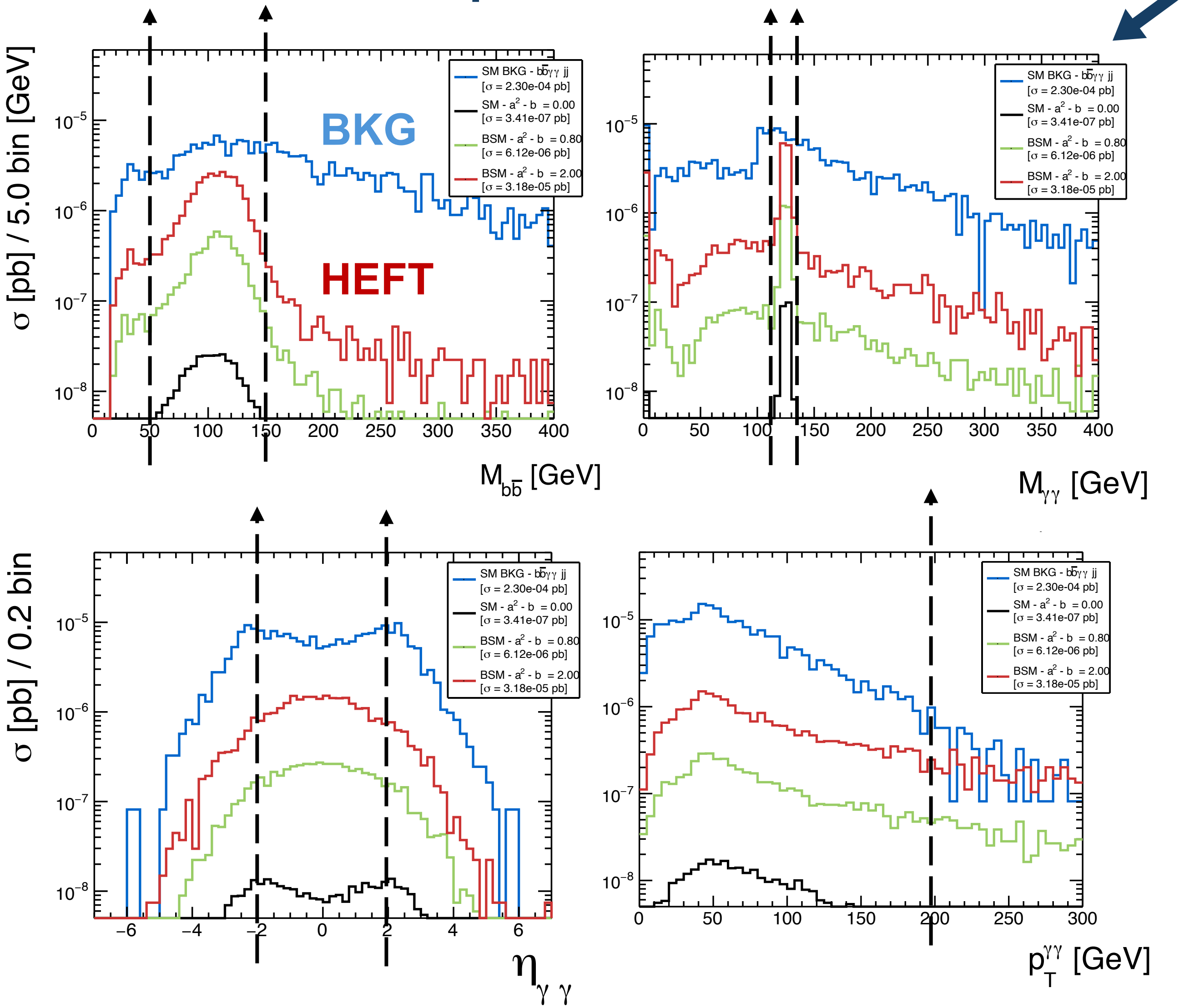

Further selection (sequential) cuts:

VBF criteria

≥ 2 light jets: $P_{T,j} > 20$ GeV, $2 < \lvert\eta_j\rvert < 5$
VBF jet pair jj' maximizes ΔR
$\eta_j \times \eta_{j'} < 0$
$m_{jj'} > 500$ GeV

(and b-jet/γ identification)

≥ 2 "loose" photons: $P_{T,\gamma} > 18$ GeV, $\lvert\eta_\gamma\rvert < 2{,}5$
Photon pair $\gamma\gamma$ closest to $m_{\gamma\gamma} = m_H = 125$ GeV
≥ 2 "loosely" b-tagged jets: $P_{T,j_b} > 25$ GeV, $\lvert\eta_{j_b}\rvert < 2{,}5$
b-jet pair $j_b j_{\bar{b}}$ closest to $m_{j_b j_{\bar{b}}} = m_H = 125$ GeV

*same as in slide 10

$M_{\gamma\gamma}$ + $M_{b\bar{b}}$ criteria

	SM E_i	$b\bar{b}\gamma\gamma jj$ BKG E_i
$120 < M_{\gamma\gamma} < 130$ GeV	55%	6%
$50 < M_{b\bar{b}} < 150$ GeV	89%	45%

STRATEGY I

OPTIMAL FINAL CUT IN $\eta_{\gamma\gamma}$

$\eta_{\gamma\gamma}$ criteria

	SM E_i	$b\bar{b}\gamma\gamma jj$ BKG E_i
$-2 < \eta_{\gamma\gamma} < 2$	60%	59%

STRATEGY II

OPTIMAL FINAL CUT IN $P_T^{\gamma\gamma}$

$P_T^{\gamma\gamma}$ criteria

	SM E_i	$b\bar{b}\gamma\gamma jj$ BKG E_i
$P^t_{\gamma\gamma} > 200$ GeV	8%	3%

Sensitivity to ($a^2 - b$) in $pp \to HHjj \to b\bar{b}\gamma\gamma jj$ production at HL-LHC

SENSITIVITY CAN BE LARGE WITH CUTS REQUIRING HIGH TRANSVERSALITY OF $\gamma\gamma$ PAIR

Sensitivity formula: $$S = \sqrt{-2\left((N_S + N_B)\log\left(\frac{N_B}{N_S + N_B}\right) + N_S\right)}$$

STRATEGY I ⇒ OPTIMAL CUT IN $|\eta_{\gamma\gamma}| > 2$

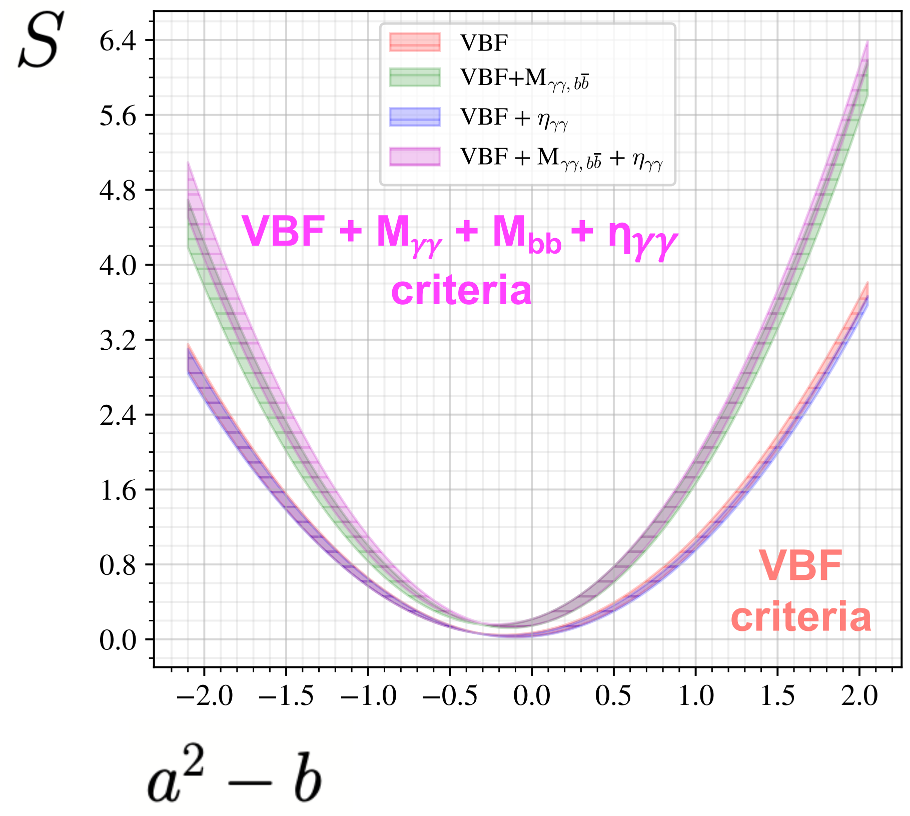

STRATEGY II ⇒ OPTIMAL CUT IN $P_T^{\gamma\gamma} > 200$ GeV

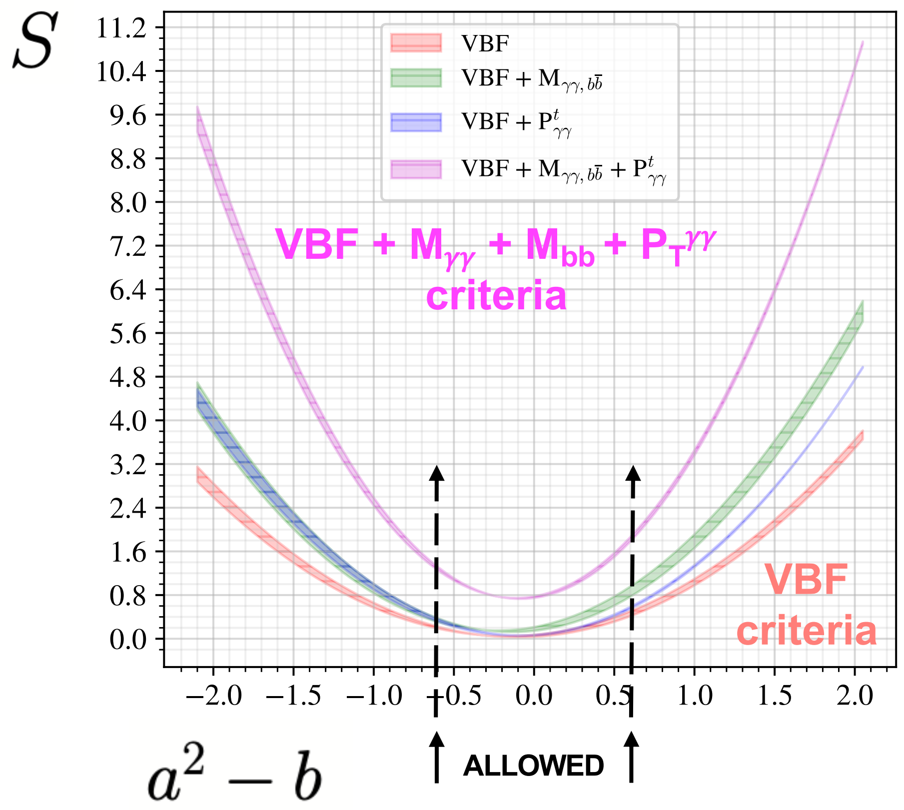

EVEN FOR $-0.6 < a^2 - b < 0.6$, $S \simeq 2$ IMPROVES PRESENT SENSITIVITY USING JUST ONE CHANNEL

Conclusions

- ★ We have explored the sensitivity to $(\kappa_V^2 - \kappa_{2V})$ at **HL-LHC** by means of a single channel **pp** $\to$ **HHjj** $\to$ **b$\bar{\text{b}}\gamma\gamma$jj** for the first time.

- ★ We have found a high sensitivity to this combination.

- ★ The determination of this combination will provide some hints on new BSM Higgs physics.

- ★ The predictions presented here are performed within the HEFT, which is the most appropriate EFT to discuss BSM HVV and HHVV interactions.

BACKUP SLIDES

Comments on κ_3 and κ_4

1) κ_4 does not enter in **pp → HHjj**

2) $\kappa_3 = \kappa_\lambda$ does enter in **pp → HHjj**

but the effect of $\kappa_3 = 1$ is much lower than the effect of $(a^2 - b) \neq 0$.

- $\kappa_3 \neq 1$ is only marginaly visible closer to the HH threshold (i.e. close to $M_{HH} \simeq 2m_H$)

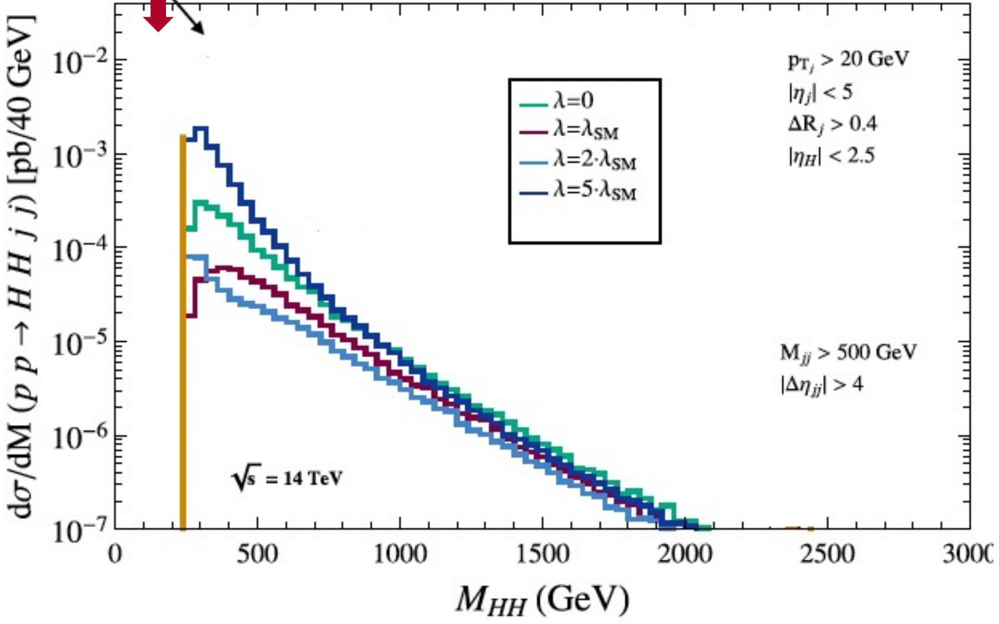

Taken from E. Arganda et al. / Nuclear Physics B 945 (2019) 114687

- $(a^2 - b) \neq 0$ is clearly visible in the whole M_{HH} (or $M_{b\bar{b}\gamma\gamma}$) range

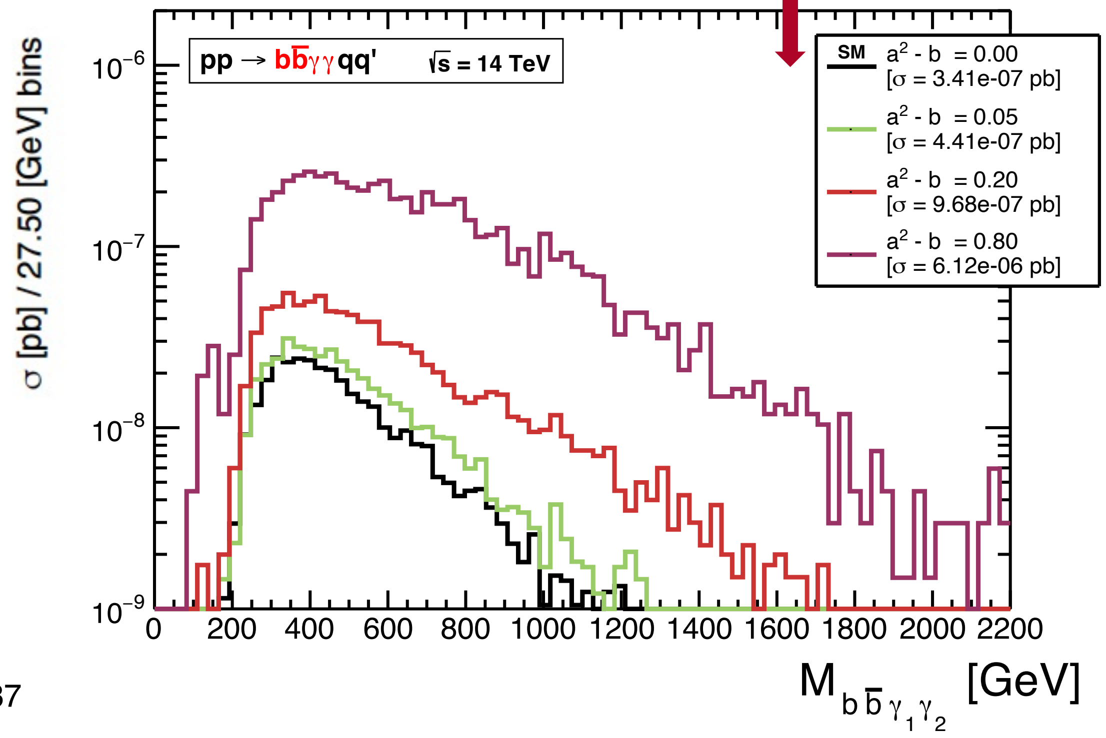

WW → HH high energy total unpolarized cross-section with SM case

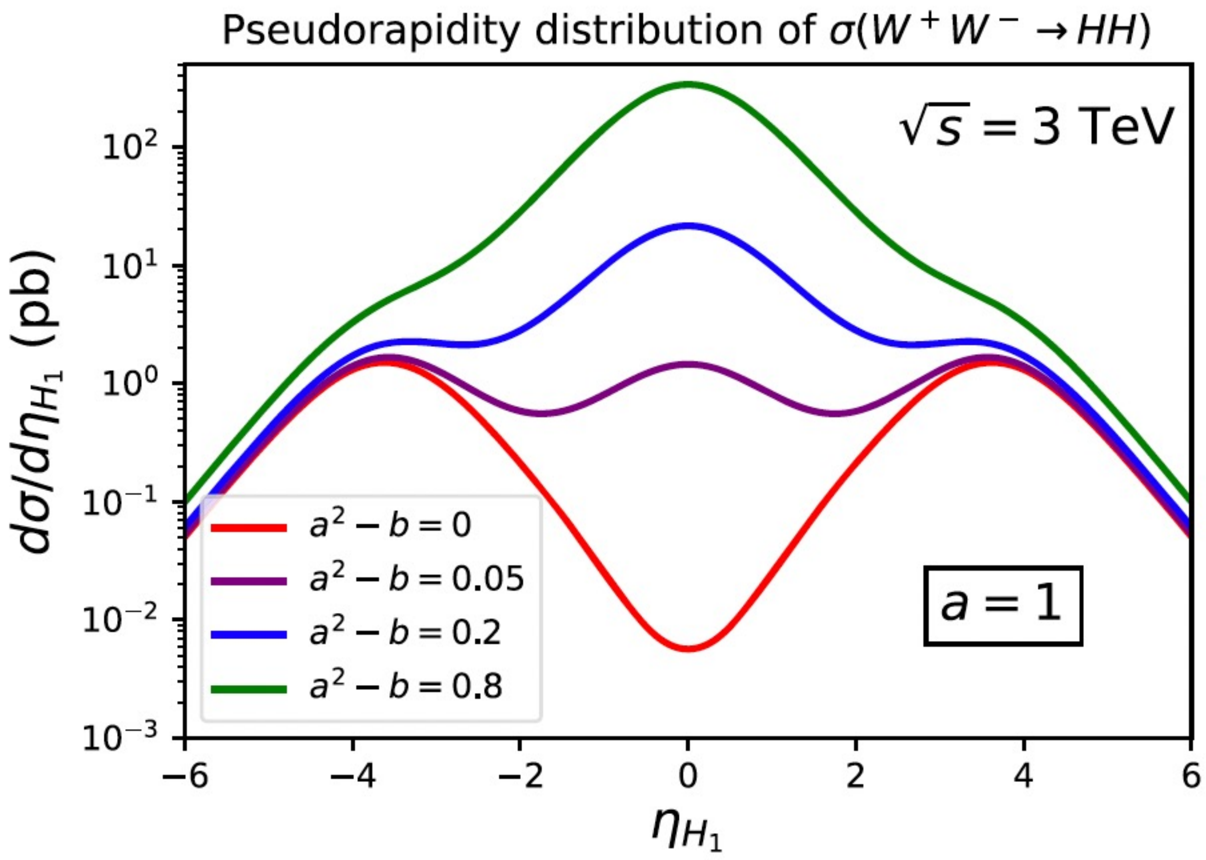

Details on the HEFT results on the total xsection σ(pp → HHjj)